

CASE STUDY OF OLD STEEL RIVETED RAILWAY TRUSS BRIDGE: FROM MATERIAL CHARACTERIZATION TO STRUCTURAL ANALYSIS

ANDRZEJ AMBROZIAK*, MACIEJ MALINOWSKI

*Faculty of Civil and Environmental Engineering,
Gdansk University of Technology, Gdańsk, Poland*

Received 14 February 2023; accepted 29 June 2023

Abstract. The structural analysis of an old steel riveted railway truss bridge located over the Maruska River on the Działdowo – Olsztyn, Poland railway line is performed in this paper to check its behaviour under today's railway loads. The mechanical properties of construction steel extracted from the old steel bridge are investigated by tensile tests, impact tests through the Charpy pendulum impact V-notch, and an optical emission spectrometer. Structural analysis exhibits that the steel bridge requires proper structural bridge improvements to meet today's load requirements in terms of bearing capacity and serviceability state. The paper begins with a wide survey of literature carried out on the investigation of steel riveted railway bridge subject matter. This paper can provide scientists, engineers, and designers with an experimental and structural basis in the field of old steel riveted railway truss bridge construction.

Keywords: bridge structure, FEM, mechanical properties, steel riveted bridge, structural health assessment, truss bridge.

* Corresponding author. E-mail: ambrozan@pg.edu.pl

Andrzej AMBROZIAK (ORCID ID 0000-0002-7735-7863)
Maciej MALINOWSKI (ORCID ID 0000-0002-8266-1034)

Copyright © 2023 The Author(s). Published by RTU Press

This is an Open Access article distributed under the terms of the Creative Commons Attribution License (<http://creativecommons.org/licenses/by/4.0/>), which permits unrestricted use, distribution, and reproduction in any medium, provided the original author and source are credited.

Introduction

Truss bridges are one of the most popular types of bridges (Siwowski et al., 2020). Steel riveted bridges represent an important part of the cultural and constructive heritage of the past century. Many iron and steel riveted bridges are considered historically significant and need to be restored and preserved and are still in service. Riveted construction was the method used for building up members and for the connection of one member to another. Rivets were widely used as mechanical fasteners in truss bridges constructed after the 1900s through the 1970s when high-strength bolts replaced the use of rivets. Decades-old riveted steel bridges that are still in service need to be reassessed. Of fundamental importance are the realistic assessment of the technical conditions, state of fatigue, and bearing capacity of bridge structures, which is instrumental in defining the scope of the reconstruction or repair process. Reconstruction and renovation of old bridges and adaptation to new loads are very often complex issues requiring not only the experience of civil engineers but also that of the scientific community.

The present study is aimed at the structural analysis of the old steel railway riveted truss bridge based on mechanical properties determined through laboratory tests. Structural analysis was a part of an expert opinion, required to check whether the old steel riveted bridge has an adequate bearing capacity face to present railway loads and requirements. The possibility to extend its service life is also investigated. The paper can be treated as an extension of the authors' former investigations performed on old concrete bridges and structures (Ambroziak et al., 2019; Ambroziak & Malinowski, 2021) to old steel riveted bridges. This paper gives scientists, engineers, and designers a case study on an old rivet steel bridge examined from the properties of the materials – by testing samples in a lab – to the structural behaviour and structural analysis – by finite-element modelling which is preceded by a wide literature review. The literature review gives a view of the performed investigation and indicates new and future directions of investigations on riveted steel bridge constructions.

1. Literature review

In the literature, it is possible to find many interesting investigations related to steel riveted bridges. Malinowski et al. (2017) described the history of the 160-year-old wrought-iron lattice truss bridge in Tczew, Poland regarding the two emerging ideas of the reconstruction. Michalak & Eckert (2018) described the historic steel bridge built in 1903 in Stany,



Poland. Ocel (2021) presented a view of historical steel bridge design with an emphasis on the evolution of the steel itself. A timeline of major design changes, such as welding and bolting, composite design, and fatigue design, is also described. Haghani et al. (2012) performed comprehensive reviews of fatigue damage cases in more than 100 bridges. Jakiel & Bajno (2018) presented the characteristics of the bridge along with its historical background, concentrating mainly on the results of inspections of the structure in the context of assessing its technical condition.

Different diagnostics and damage detection methods for steel bridges are developed and used. Zobel et al. (2016) investigated the structural damage method and restoration method after the Łazienkowski bridge fire in Warsaw, Poland. Marchewka et al. (2020) presented the framework for noninvasive diagnostics of the riveted steel truss Fitzpatrick Bridge (located in the city of Tallassee, Alabama, in the United States) using unmanned aerial vehicles. Goszczyńska et al. (2013) applied an acoustic emission method for the assessment of a steel riveted bridge in Sandomierz, Poland. The results made it possible to evaluate the technical condition of the bridge under service load. Bień & Salamak (2022) described the classification of Bridge Management Systems to show the history of creating such systems and indicated the expected directions of their development, taking into account changing challenges and integrating new developing technologies. Walia et al. (2015) described the damage identification in an existing 100-year-old deck-type steel truss bridge using frequency- and time-frequency-based approaches. Brühwiler et al. (2013) conducted long-term monitoring of the structural elements of a 115-year-old riveted railway bridge structure.

Many researchers performed expert opinions on the technical condition, and evaluation of the fatigue life, and carried out different propositions and descriptions of steel riveted bridge strengthening and reconstruction ways. Siwowski (2015) performed a fatigue assessment of an existing riveted truss bridge. Pipinato et al. (2012) performed the structural assessment of the Adige Bridge, Italy which has been serviced since 1886. Holzinger et al. (2002) described methods for strengthening an old arch-truss bridge located in Austria. Malešev et al. (2016) presented the assessment of a steel bridge over the Bosut River in Serbia which included: a detailed visual inspection of all accessible elements with the registration of defects and damages characteristics, evaluation of incorporated materials quality, determination of the depth of cracks in the river piers and structural calculation. Łagoda & Łagoda (2009) described strengthening a steel bridge with a riveted framework across the Vistula River in Poland with carbon fibre-reinforced polymer strips. Wang et al. (2007) performed a fatigue and fracture evaluation of a



70-year-old steel bridge. Hołowaty & Wichtowski (2022) investigated the technical condition of 13 steel bridges built between 1873 and 1890 and 17 bridges from the years 1907 to 1983. Vůjtěch et al. (2021) presented a progressive method of strengthening the 113-year steel bridge in the Czech Republic with the use of a Fe-Mn-Si shape memory alloy.

Different methodological approaches and methods are proposed to evaluate the structural condition of steel bridges, the fatigue life, and the structural health monitoring system. Sangiorgio et al. (2022) proposed a methodological approach to develop an analytical fault tree based on the calibration of a numerical FEM model for historical steel truss bridges. Boukezzi et al. (2021) showed that methods based on a semi-probabilistic approach could not be considered a good tool for existing steel railway bridge evaluation. Helmerich (2013) formalized the existing knowledge in the specific domain of riveted bridges using standardized terms and semantic relations between them. Rakoczy (2021) performed fatigue safety verification of riveted steel railway bridges using a probabilistic method and standard S-N curves. Nowak et al. (2017) researched bridge construction elements using an acoustic emission method. Kołakowski et al. (2011) presented the results of in situ investigations of a railway truss bridge in the context of structural health monitoring. Goszczyńska et al. (2014) assessed the technical state of large-size steel structures under cyclic load with the acoustic emission method called identification of active damage processes.

Numerical analysis and simulations are widely conducted on steel riveted bridges. Salem & Helmy (2014) analytically investigated the cause of the collapse of the truss-arched I-35 Bridge in Minnesota using the applied element method. Chen et al. (2012) performed finite element simulation and its updating for the 104-year-old Waibaidu Bridge. Imam et al. (2005) presented fatigue-related results obtained from finite element analyses of a typical riveted railway bridge. Jukowski et al. (2018) verified various numerical models concerning the measurements of a steel bridge subjected to dynamic loading. Kołakowski et al. (2013) focused on the utilization of experimental data for refining a numerical model of the steel truss bridge as well as on tests of dynamic excitations using a controlled hydraulic shaker and passing trains. Siekierski (2015) compared the modified beam-element modelling of a scaled bridge truss girder to regular hybrid modelling that employs beam elements to model members and shell elements to model joints.

Different rehabilitation and strengthening methods are developed and used. Lima et al. (2008) described the rehabilitation of a 100-year-old riveted steel through-truss bridge in Canada. Kääriäinen & Pulkkinen (2002) described the process of the rehabilitation of the Tornionjoki Steel Truss Bridge. Siwowski (2013) described rehabilitation

works on the five-span continuous Warren-type steel truss bridge built in 1961. Gheitasi et al. (2022) showed a rehabilitation highlighting different aspects of design and construction that includes partial disassembly, temporary relocation, and retrofit of the 133-year-old historic steel truss bridge. Heydarinouri et al. (2021) described a retrofit system for strengthening the stringer-to-floor-beam double-angle connections in a 92-year-old riveted railway bridge in Switzerland, using prestressed CFRP rods.

Many laboratory investigations on old steel bridge elements are conducted. Nguyen et al. (2015) evaluated corrosion at the contact surface on gusset plate connections of a steel truss bridge. Leonetti et al. (2020) developed a procedure to measure the clamping force in hot-driven rivets and measured the clamping force of rivets from a bridge in service for 70 years. Martín-Sanz et al. (2019) tested at laboratory facilities a riveted steel bridge constructed in 1893 and decommissioned after rehabilitation via the addition of the UHPFRC slab. Siekierski (2016) carried out lab testing of a scaled bridge truss girder and investigated stress distribution in a gusseted joint. Bacinskas et al. (2013) investigated the structural condition and the behaviour of the riveted steel truss bridge with the aid of full-scale static and dynamic testing. Pipinato (2010) performed a series of diagnostic tests on a two-lane, historical railway steel-girder bridge, in service from 1918.

Laboratory tests on full-scale steel bridge elements are also performed. Aktan et al. (1994) performed a series of nondestructive and destructive tests for two decommissioned 80-year-old steel truss bridges. Wang et al. (2012) performed a series of tests including material mechanics, fracture, and fatigue properties on an original steel angel cut off from a riveted truss Lanzhou Zhongshan Bridge from 1909. Nagavi & Aktan (2003) presented nonlinear modelling and analysis of a decommissioned steel truss bridge in Franklin County, Ohio that was tested to failure.

Experimental, analytical and numerical analyses are also carried out. Cavadas et al. (2013) performed an experimental and numerical analysis regarding the structural assessment of the Eiffel Bridge, Portugal. The effectiveness of the strengthening of the top chords was verified based on the strain measurements. Stamatopoulos (2013) perform an experimental and analytical study of a 19th-century riveted steel truss railway bridge and proposed the necessary strengthening of the bridge. Marques et al. (2014) described the experimental and numerical studies to evaluate the local fatigue effects of the Trezói Bridge (metallic riveted bridge), in Portugal. Yilmaz et al. (2022) evaluated the safety index of a steel girder railway bridge situated in Turkey with a fully probabilistic simulation approach.



Determinations of construction material properties of steel riveted bridges are widely also performed. Vélez et al. (2021) examined old steel (nearly or over 100 years old) behaviour and its fatigue assessment taken from seven Spanish conventional rail network bridges. Kowal & Szala (2020) investigated the material properties of an over 120-year-old steel railway bridge and compared its mechanical and chemical properties to modern steel. Hołowaty & Wichtowski (2015) determined the properties of steel in a railway bridge constructed in 1887. Schabowicz (2021) proposed and organised as a means to present recent developments in the field of testing materials in civil engineering. Hołowaty and Wichtowski (Hołowaty & Wichtowski, 2013; Wichtowski & Hołowaty, 2011) performed an analysis of the chemical composition, determination of hardness and toughness, along with yield strength and ultimate strength of cast steel from four railway truss bridges built in 1875. Hołowaty (2018) investigated the properties of high-tensile steels in historical railway bridges. Collette et al. (2014) investigated the geometry and metallography of wrought-iron rivets dismantled from four bridges and buildings built in the 1880s–1890s. Kossakowski (2016), (2021) presented the laboratory testing results of the strength of structural steel taken from a railway bridge. Kossakowski (2013) presented the results of the research on the fatigue strength of steel sampled from a railway bridge exploited over a hundred years.

The problem of the corrosion rate and assessment of steel degradation are analysed and investigated. Cywiński (1992) investigated the corrosion rate of structural steel in old bridges. Jang et al. (2013) estimated the corrosion level in a historic steel-truss bridge using model updating. Chmielewski & Muzolf (2021) presented the problem of assessing the degradation process of a selected railway steel bridge. Gocál & Odrobińák (2020) investigated the impact of the atmospheric corrosion of structural steel on the load-carrying capacity of old riveted bridge structures.

It can be mentioned that steel riveted constructions are still widely tested and investigated by engineers, researchers, and scientists. The development of welding changed the joint connection of steel members and gave possibilities for the design of new types of steel structures. The beginning application of welding to steel bridges was in the 1930s (Alencar et al., 2019). The first arc-welded bridge in Europe was designed by Bryła (Hołowaty, 2018) and was erected near Łowicz, Poland. The rivet joints were replaced systematically by welding or bolt connections. Nevertheless, decades-old steel bridges that are still in service need to be reassessed, rebuild or reconstructed.

2. Materials and methods

The railway truss riveted bridge is located over the Maruska River on the Działdowo-Olsztyn, Poland railway line (see Figures 1 and 2). The railway line was constructed in 1888, but the year of the bridge construction is the early 20th century. The load-bearing structure of the bridge is a freely supported truss span with a theoretical span of 39.6 m, double-girder, with overhead driving, and with an open carriageway. The main girders are parabolic trusses with a curved lower chord – a variable height of the truss (6.60 m in the middle of the span), with a W-type grating with posts and hangers (see Figure 1). The transverse spacing of the truss girders is 3.10 m. The lower chords with open cross-sections, two-branch, braced with battens, are made of vertical steel sheets 380 mm high, reinforced with additional vertical sheets, and L120×120×12 angle bars located at the edge of the vertical steel sheets. The upper chords are made with a hat-shaped cross-section (open at the bottom) made of two C260 channels reinforced from above with horizontal 440×12 mm steel sheets (see Figure 3). The posts and

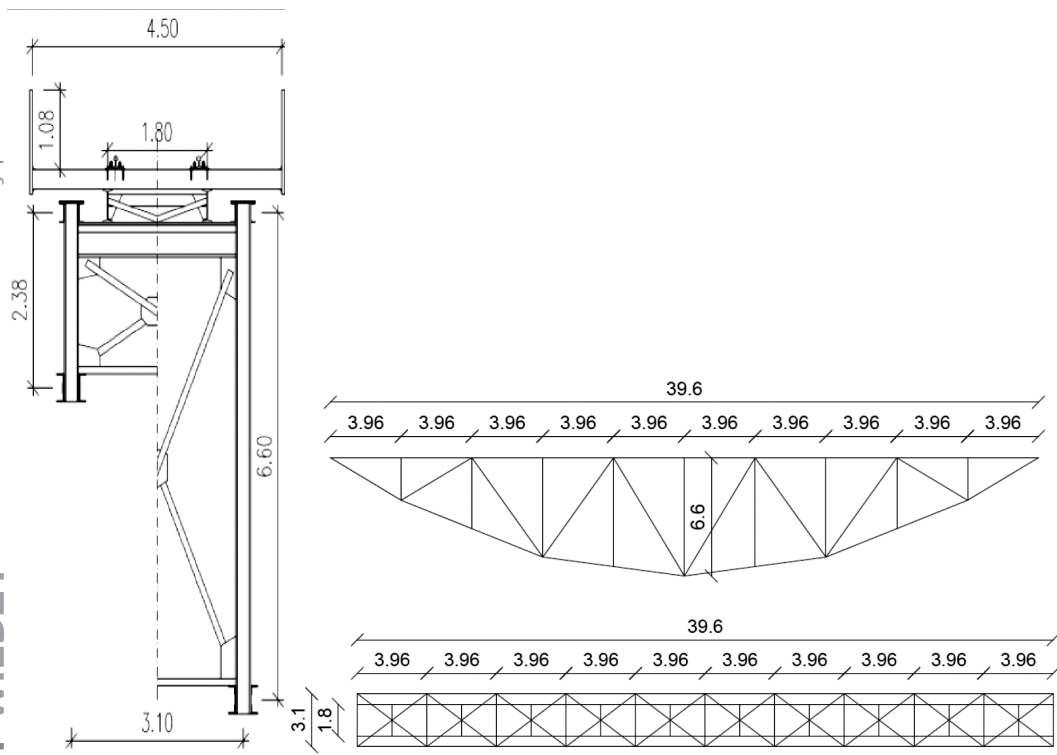


Figure 1. Bridge cross-section and scheme view

a) side view



b) bottom view



c) bottom joint



d) support joints



Figure 2. Railway truss bridge

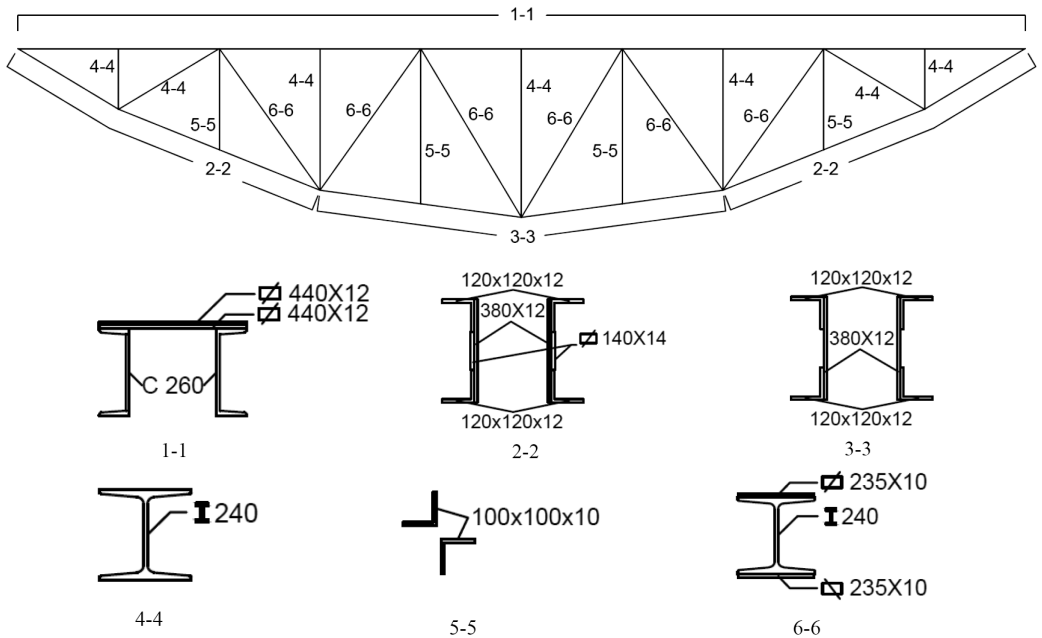


Figure 3. Bridge scheme with member cross-sections

some diagonals are made of HEB240 rolled I-beams, the other diagonals (in the central part of the span) are made of HEB240 rolled I-sections reinforced with 235×10 mm sheets, and the hangers – as open sections are made of two 100×100×10 mm angle bars with battens. The bridge deck is made of a grid of stringers with a spacing of 1800 mm and a cross girder with a spacing of 3960 mm. Stringers (rolled I-beams T450) and cross-beams (I-beams rolled T475) are connected only through angles 160×160×19 mm connecting the webs of both beams. The X-type upper wind girder with T-beam diagonals in the plane of the lower chords of the cross girder and vertical transverse braces with X-type grating located in the places where the truss posts are located.

In the laboratory tensile tests, the strength-testing computer-operated machine of Zwick/Roell 250 type was applied. The hydraulic jack was computer-operated by the TextExpert program. The values of displacement and force on the hydraulic jack were recorded. The tensile testing of steel samples was performed according to ISO 6892-1 (ISO, 2019) standard, where the method for tensile testing of metallic materials was specified.

The assessment of impact toughness and determining impact transition temperature were performed by using a computer-operated Zwick/Roell 5111 hammer. The hammer Zwick/Roell 5111 executed an impact test through the Charpy pendulum impact V-notch according to standard ISO 148-1 (ISO, 2016). Cooling of samples was performed in a cooler using liquid nitrogen. ISO 148-1 standard specifies the Charpy pendulum impact test method for determining the energy absorbed in an impact test of metallic materials.

The optical emission spectroscopy technique was used to perform an old steel sample analysis (Sanekata et al., 2021). A spectrometer was equipped with a sparking chamber under an argon atmosphere. Analytical channels have been installed for the following elements: C, Si, Mn, P, S, Cr, Mo, Ni, V, Cu, and Al in metal samples. The steel samples ablated were excited in the argon plasma generated by the sparks. The optical emission spectrometer is easy to use and maintain and it provides the fastest determination of all the elements with high accuracy and precision for applications in spectral studies.

3. Laboratory test results and discussion

Based on the performed laboratory test, the values of the upper yield point, tensile strength limit and impact resistance are determined in Table 1. The Regulations on the Construction and Maintenance of Road Bridges (*Rules for the Construction and Maintenance of Road Bridges*,



1926) indicated 235.44 MPa (2400 kg/cm²) for the yield strength of cast steel. Temporary regulations for the construction and maintenance of road bridges, issued by the Ministry of Public Works on 4 March 1920 (Bryła, 1924), indicate that the breaking strength for cast steel should be equal to or greater than 362.9 MPa (3700 kg/cm²) and less than or equal to 441.4 MPa (4500 kg/cm²), with proportional limit and yield strength equal to 196.2 MPa (2000 kg/cm²) and 235.4 (2400 kg/cm²), respectively. The standard PN-B-195 (PKN, 1945) allowed for the use of structural steel with yield strengths equal to 235.4 MPa (2400 kg/cm²). The PN-B-03200 (PKN, 1951) standard for the design of steel structures allows for steel construction usage with a breaking strength from 362.9 MPa (3700 kg/cm²) to 441.4 MPa (4500 kg/cm²) and yield strength equal to 225.6 (2300 kg/cm²). The material parameters for wrought steel and cast steel according to the International Union of Railways UIC guidelines (UIC, 1986) can be assumed as: tensile strength $R_m = 320\text{--}380$ MPa; yield point $R_e = 220$ MPa, modulus of elasticity $E = 200$ GPa and modulus of rigidity $G = 70$ GPa. According to the performed laboratory tests, the value of the upper yield point (223 ± 3 MPa) and tensile strength limit (354 ± 4 MPa) is correlated with guidelines issued in the period of bridge construction.

The absorbed energy for a V-notch test piece using a 2 mm striker (KV_2) is given in Table 1. The impact toughness in temperatures -20 °C and -40 °C are 9.4 J and 3.9 J, respectively. The obtained low values of impact toughness can be treated as normal for the cast steel. This fact cannot directly indicate that old cast steel is susceptible to brittle fracture (Hołowaty & Wichtowski, 2015). Investigations on cast steel by more detailed fracture mechanics methods indicated that cast steels had generally a good impact toughness (Sieber & Stroetmann, 2013).

Based on the optical emission spectroscopy technique, the chemical element compositions of the old steel are shown in Table 2. The obtained chemical element composition is compared with chosen results given in the literature. Bryła (Bryła, 1924) indicated that three types of steel

Table 1. The mean values of the upper yield point, tensile strength limit and impact resistance

Properties	Values
R_{eH} – upper yield point	223 MPa
R_m – tensile strength limit	354 MP
Impact toughness, temp. -20 °C	9.4 kV2/J
Impact toughness, temp. -40 °C	3.9 kV2/J



were used in construction in the 1920s: cast iron with a carbon content of more than 2.3%, welded steel with a carbon content of 0.1–0.5% and cast steel with a carbon content of 0.05–0.25%, where the cast steel was the main type of steel used for construction purposes. The chemical composition and comparisons indicate that the old steel belongs to the group of cast steel.

Based on the determined chemical compositions, the metallurgical and mechanical weldability of old steel can be verified (Adamiec & Dziubiński, 1995; Tasak & Ziewiec, 2009; Wichtowski, 2014). The carbon equivalent for cold cracking, heat-affected zone hardness and hot cracking resistance is specified. The carbon equivalent is a measure of the tendency of the weld to form martensite on cooling and to suffer a brittle fracture (Tomków & Tomków, 2019). Cold cracking is generally recognized as being caused by excessive restraint of the joint, or by martensite formation as a result of rapid cooling (Nam et al., 2021). The welded joints must have the relevant plasticity and toughness within the heat-affected zone (Krawczyk et al., 2022). The critical hardness of 350 *HV* often quoted for C-Mn steels can be applied to other ferritic steels as a reasonable guide to susceptibility to cracking, but it should not be regarded as an absolute criterion (Croft, 1996). The hot cracking susceptibility (*HCS*) parameter describes susceptibility to hot cracking. When *HCS* > 4, the hot cracking occurs; if 2 < *HCS* < 4 the hot cracking may occur, and in the case of *HCS* < 2 steel is resistant to hot cracking.

Table 2. Chemical compositions of the old steel specimens

Chemical elements	Specimen 1	Specimen 2	Mean values	Wrought steel (Wichtowski & Hołowaty, 2011)	Cast steel (Hołowaty & Wichtowski, 2015)	Mild steel (Hołowaty, 2017)
C	0.08	0.08	0.08	0.018 to 0.30	0.03 to 0.35	0.03 to 0.35
Si	< 0.05	< 0.05	< 0.05	0.10 to 0.33	traces to 0.18	traces to 0.18
Mn	0.47	0.46	0.465	traces to 0.33	0.04 to 0.75	0.04 to 0.18
P	0.037	0.035	0.036	0.02 to 0.46	0.004 to 0.16	0.004 to 0.16
S	0.032	0.035	0.0335	0.01 to 0.06	0.004 to 0.09	0.004 to 0.115
Cr	< 0.01	< 0.01	< 0.01		0.007 to 0.014	
Mo	< 0.01	< 0.01	< 0.01			
Ni	0.01	0.01	0.01		0.03 to 0.04	0.03, 0.04
V	< 0.01	< 0.01	< 0.01			
Cu	0.09	0.09	0.09		0.11 to 0.14	0.11 to 0.14
Al	< 0.007	< 0.007	< 0.007		0.01 to 0.02	0.01 to 0.02

The carbon equivalent value guideline by the International Institute of Welding is given by the following equation:

$$C_e = C + \frac{\text{Mn}}{6} + \frac{\text{Cr} + \text{Mo} + \text{V}}{5} + \frac{\text{Ni} + \text{Cu}}{15} = 0.17\% < 0.34\%. \quad (1)$$

The carbon equivalent for cold cracking is determined as:

$$C'_e = C + \frac{\text{Mn}}{6} + \frac{\text{P}}{2} + \frac{\text{Mo}}{4} + \frac{\text{Ni}}{15} + \frac{\text{Cr} + \text{V}}{5} + 0.0024 \times t = 0.24\% < 0.4\%, \quad (2)$$

where $t = 17$ mm is the thickness of the HEB flange.

The heat-affected zone (HAZ) hardness is derived as:

$$HV_{\max} = 1200 C'_e - 200 = 76HV < 350HV$$

$$HV_{\max} = 90 + 1050 C + 47 \text{ Si} + 75 \text{ Mn} + 30 \text{ Ni} + 31 \text{ Cr} = 212HV < 350HV. \quad (3)$$

Following, the hot cracking sensitivity is calculated:

$$HCS = \frac{C \left(S + P + \frac{\text{Si}}{25} + \frac{\text{Ni}}{100} \right)}{3\text{Mn} + \text{Cr} + \text{Mo} + \text{V}} \times 1000 = 4.02\% > 4.0\%. \quad (4)$$

The tested old steel is weldable because C_e is 0.17% and is lower than 0.34%, the amount of phosphorus and sulfur is lower (for each of these components) than 0.05% and the amount of manganese is lower than 1%, and silicon from 0.5%. The steel is unburdened due to trace amounts of silicon $\text{Si} < 0.05\%$. The steel is susceptible to hot cracking as $HCS > 4\%$ and $\text{Mn}/\text{S} = 13.88$ are in the hot weld cracking zone. In the case of old steel welding, precautions should be taken, e.g., controlling the arc energy or low preheating.

4. Structural analysis

4.1. Description of FEM model

The three-dimensional finite element model of the old steel riveted truss bridge is built (see Figure 4). The cross-sections of the bridge members are taken according to measurements of on-site vision (see Figure 3). The SOFiSTiK structural engineering system is applied in numerical calculations. The SOFiSTiK software is frequently used in the design and analysis of bridge structures (Banas & Jankowski, 2020; Malinowski et al., 2018; Zoltowski et al., 2022). The 3D beam (B3D) finite elements (FE) are applied in the FEM model of the bridge. The finite elements adopted in the calculation are 2-node 3D beam elements of the Timoshenko type, C0 class with linear shape functions. The FEM



model of the old bridge is meshed by 2914 3D beam elements, the model includes 2804 nodes with 8 support constraints. In the FEM model, non-flexible connections of elements in nodes without gusset plates are taken into account. The cross-sections of structural elements are treated as homogeneous, without taking into account the susceptibility of riveted joints. In other cases, where detailed rivet connections have to be investigated, the local FEM models of the most critical connections must be applied with contact and friction between the individual parts of the connection as well as the rivet clamping force is included (see, e.g., Bertolesi et al., 2021; Correia et al., 2021; de Jesus et al., 2014; Marques et al., 2018).

The following structural conditions are taken into account in the calculation model: the mutual position of individual structural elements (eccentricity); non-flexible nodes of truss girders; and geometric and material parameters adopted based on laboratory tests and measurements and based on the results of the tests carried out and the assumptions made.

In the present structural analysis of the old steel riveted bridge, the basic and additional loads are taken into account. It is assumed that basic loads are the following:

- permanent loads – self-weight of the load-bearing structure and equipment elements; the values of permanent loads were adopted based on own supplementary measurements;
- standard railway class load LM71 according to PN-EN 1991-2: 2007 (PKN, 2007) (also like in PN-S-10030 (PKN, 1985)), taking into account the appropriate dynamic factor;
- standard railway service load of classes C2 and D4 according to PN-EN 15528: 2022 (PKN, 2022) with dynamic coefficient values appropriate for given speeds according to PN-EN 1991-2: 2007

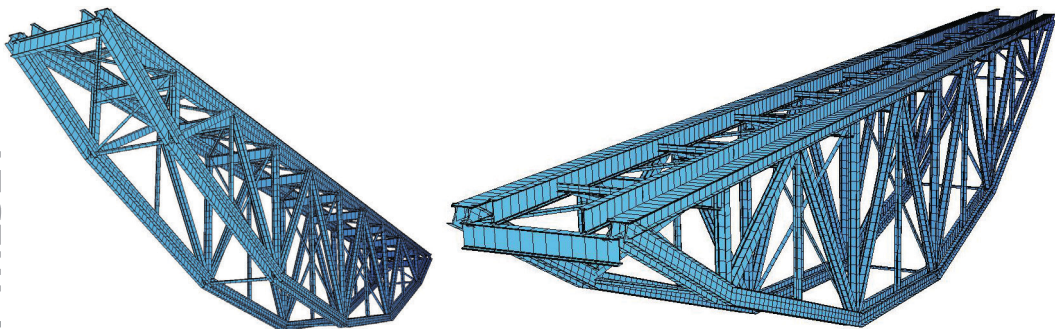


Figure 4. 3-D views of the FEM model



(PKN, 2007) and with a partial safety factor equal to 1.45 applied to the actions;

and additional loads are the following:

- load from traction and braking forces on the bridge according to PN-EN 1991-2: 2007 (PKN, 2007);
- load from nosing forces according to PN-EN 1991-2: 2007 (PKN, 2007);
- wind load for unloaded structure and loaded with rolling stock;
- load with temperature increases.

In some countries, the load and action values for the design of new railway bridges are different from the loads and actions for existing bridges. For example, in Germany, the requirements for existing railway bridges are guidelines (DB AG, 2000; DB Netz AG, 2010; Steffen et al., 2023). The Polish Construction Law does not provide straightforward guidelines for determining load and actions on historic railway bridges. The reliability of existing bridge structural elements and their load-carrying capacities is verified and determined using the partial safety factors method (Leander et al., 2015; Vičan et al., 2016). Nevertheless, due to the age of the bridge structure and the dimensioning methods in force at the time of its design, the degree of effort was checked and the load capacity was estimated using the allowable stress method (Apanas et al., 2018; D-64, 1955; UIC, 1986). The choice of the method was also imposed by the orderer for whom the expert opinion was prepared. Internal forces and stresses were calculated for the values of characteristic loads (PKN, 1985, 2007, 2022).

4.2. Results of structural analysis

Based on the carried out laboratory tests of the old steel, the following parameters were adopted for the performed structural analysis:

- The upper yield point $R_{eH} = 223$ Mpa, and the tensile strength limit $R_m = 354$ Mpa;
- According to the recommendations of the technical standard (D-64, 1955) and UIC guidelines (UIC, 1986), the permissible stresses were assumed at stretching, compression, and bending as follows: $\sigma_{lim}^I = 143$ MPa, $\sigma_{lim}^{II} = 176$ MPa;
- allowable stresses in a complex state of stresses are limited to $\sigma_{lim}^I = 157.3$ MPa, $\sigma_{lim}^{II} = 193.6$ MPa.

Additionally, the bridge construction elements were checked for the analysed load combinations, assuming the value of design strength of steel based on the recommendations of the PN-S-10052 (PKN, 1982) standard and the actual limit value plasticity R_e of structural steel determined based on laboratory tests:



- The upper yield strength $R_{eH} = 223$ MPa and the design strength of steel $R = 223/(1.15 \times 1.05) = 184.7$ MPa;
- The stress limits for the complex stress state and for checking normal stresses, taking into account the stiffness of nodes are $1.1 R = 203.2$ MPa.

The FEM numerical analysis allows for the evaluation of the internal forces and stresses acting on the steel bridge construction elements and determined their largest values (see Figure 5 and Tables A1–A8). The internal forces and displacement distribution image allow verification under the service loads and the ultimate loads on the bridge structure. Based on the obtained structural analysis results, the following conclusions can be drawn:

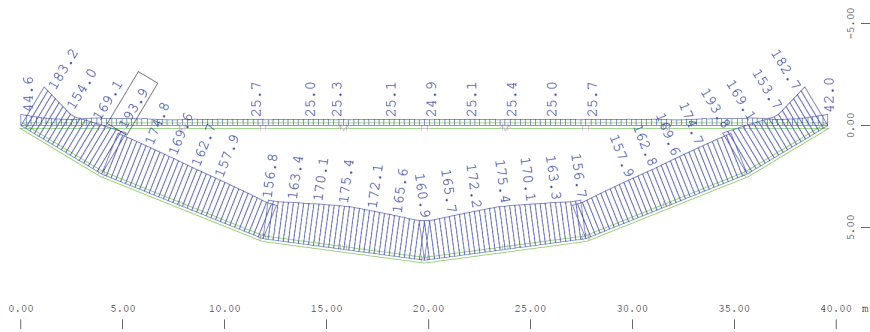
- Truss bridge girders meet the load capacity requirements for the LM71 class load according to PN-EN 1991-2 (PKN, 2007) with a coefficient $\alpha k = 1.06$ in the basic combination of loads and $\alpha k = 0.90$ in the additional load combination;
- Bridge deck elements – stringers meet the load capacity requirements for the LM71 load according to PN-EN 1991-2 (PKN, 2007) with coefficient $\alpha k = 1.40$ in the basic combination of loads;
- Bridge deck elements – cross girders meet the load capacity requirements for the LM71 load according to PN-EN 1991-2 (PKN, 2007) with the coefficient $\alpha k = 0.39$ in the basic combination of loads and $\alpha k = 0.33$ in the additional load combination;
- Truss bridge girders meet the load capacity requirements for class freight rolling stock C2 and D4 according to PN-EN 15528 with values of dynamic coefficients according to PN-EN 1991-2 corresponding to rolling stock speeds up to $V = 120$ km/h for passenger rolling stock and $V = 80$ km/h for freight rolling stock;
- The bridge deck elements (stringers and cross girders) do not meet the load capacity requirements class C2 and D4 freight rolling stock according to PN-EN 15528 with values of coefficients dynamic according to PN-EN 1991-2 corresponding to the rolling stock speed up to $V = 120$ km/h for passenger rolling stock and $V = 80$ km/h for freight rolling stock; when the maximum speed of the rolling stock is limited to $V = 50$ km/h; the elements of the bridge do not meet the load capacity conditions for the loading of freight rolling stock of class C2 and D4 according to PN-EN 15528.

To adapt to the possibility of operation for class C2 and D4 loads at the speed of the rolling stock $V = 80$ km/h, the reconstruction of the old steel bridge should be carried out in the following range:

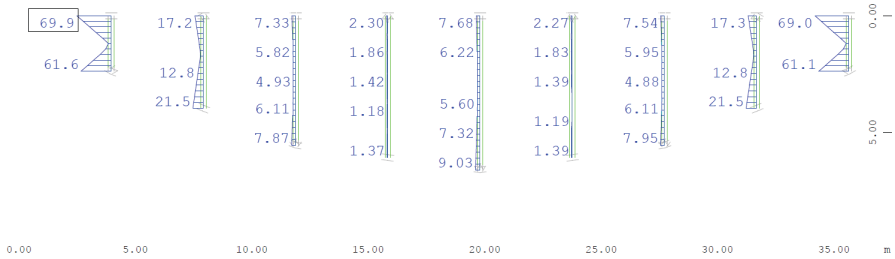
- Present stringers should be replaced by the 400HEB I-beams in the continuous beam scheme along with new oscillating braces. The application of new stringers enables the use of centring stools



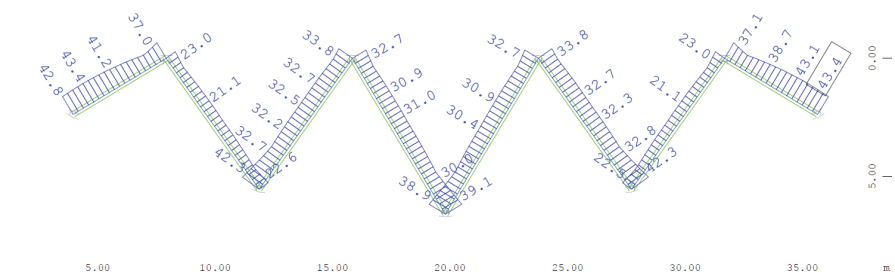
a) upper and lower chord



b) verticals



c) diagonals



d) stringer

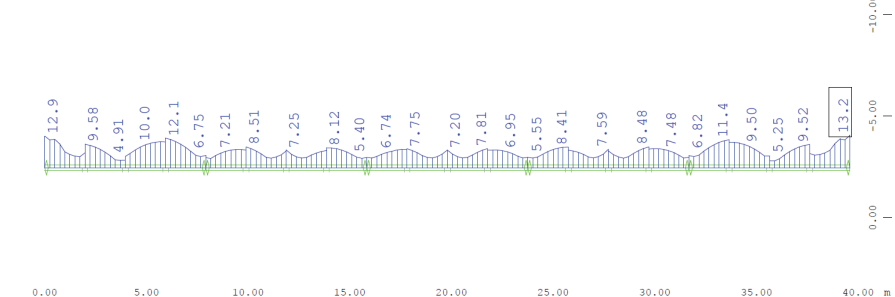


Figure 5. Characteristic stress values in the chosen bridge members for base load combination LM71, $\alpha = 1.00$ (MAX-N BEAM)

to support bridge girders (the possibility of appropriately levelling the grade line of the railway track on the bridge);

- Cross girders should be replaced by new girders with a higher load-bearing capacity;
- Diagonals of wind girders should be replaced by new ones with a higher load-bearing capacity in the first and last sections of the bridge;
- Works related to the replacement of the bridge elements should be carried out based on the design executive.

Additionally, the following maintenance must be done on the old steel riveted bridge to extend its service life:

- Completing missing rivets in the bridge structure;
- Replacement of the bridge girders on the bridge deck structure;
- Supplement or replacement of degraded steel elements of the railway bridge superstructure;
- Installation of anti-derailment railway components and fire protection sheet metal plates;
- Executing new railings or adopting existing railings to the present standard requirements and regulations;
- Cleaning the steel bridge structure by sandblasting and performing protective anti-corrosion with a suitable painting set;
- Carrying out bearing maintenance on supports;
- Removing growing vegetation and moss from the bodies of abutments, back walls, and wings;
- Cleaning and filling gaps in joints between stone blocks of supports.

Conclusions

The old riveted steel bridge over the Maruska River on the Działdowo – Olsztyn, Poland railway line was examined in this paper, from the properties of the materials – by testing samples in a lab – to the structural behaviour – by finite-element modelling. The following results are reported:

- The technical condition of the old riveted steel bridge is satisfactory. The present technical condition is the result of many years of serviceability;
- The construction of the bridge fulfils the requirements (in terms of geometry) of the railway clearance gauge GPL-1 guideline in the PKP Technical Condition (Koc, 2021; PKP, 2015);
- The bearing capacity of the structure and its useful usability are determined by the bridge deck structure;



- The steel bridge structure was made of cast steel. At low temperatures ($-40\text{ }^{\circ}\text{C}$) the old steel shows a significant reduction in impact strength, which may reduce the structure resistance to brittle cracks. The results of the spectrometric analysis of old steel are used to check the possibility of weldability;
- The present properties of old steel may differ quite significantly from the virgin properties due to steel ageing. During the time of steel ageing the material parameters change. It was observed that strength, yield point, or hardness increased, while the elongation at break and impact strength decreased;
- Internal forces for this type of bridge structures during their design period were calculated based on influence lines with an application of statically determinate systems which did not include the spatial interaction of all bridge elements, which is currently possible through the use of a 3D computational model.
- Results of static and strength calculations for the bridge structure with the new ones replaced stringers and some cross girders show that the bridge structure meets the load capacity conditions for class C2 and D4 loads according to PN-EN 15528 (PKN, 2022) at max. rolling stock speed on the facility $V = 80\text{ km/h}$.

Assessment of the load-bearing capacity of old steel bridges required individual analysis. The material parameters should be based on the current properties of the old steel and should take also into account the fact that the steel ageing continues over time (Wichtowski, 2014) and the mechanical properties of steel may be changed. In the case of beginning repair of the bridge and replacement of existing old steel bridge elements, the scope of necessary works may be increased. During construction works, other damage types or faults may appear, which are impossible to be unequivocally identified in time-detailed structural inspections. Thus, new methods, such as laser scanning, photogrammetry techniques and ground penetrating radar, have been increasingly used in terms of monitoring, inventory control and structural inspection (Kwiatkowski et al., 2020; Riveiro et al., 2013).

Assessment of old steel bridges is a key issue for managing decisions regarding the rehabilitation or replacement of existing bridge structures. The applied verification method of the reliability of the cross-sections and members of the bridge structure and their load-carrying estimation may be questionable. Nevertheless, based on the present investigation and expert opinion the old steel bridge was rebuilt and restored to service life – trains pass smoothly to this day. The present investigation shows how combining laboratory tests and numerical modelling with structural analysis contributes to the redevelopment and preservation of the old steel riveted bridge and gives it a new life for serviceability.



REFERENCES

- Adamiec, P., & Dziubiński, J. (1995). *Pękanie i trwałość napawanych części maszyn*. Wydawnictwo Politechniki Śląskiej.
- Aktan, A. E., Lee, K. L., Naghavi, R., & Hebbar, K. (1994). Destructive testing of two 80-year-old truss bridges. *Transportation Research Record*, 1460, 62–72. <https://onlinepubs.trb.org/Onlinepubs/trr/1994/1460/1460-008.pdf>
- Alencar, G., de Jesus, A., da Silva, J. G. S., & Calçada, R. (2019). Fatigue cracking of welded railway bridges: A review. *Engineering Failure Analysis*, 104, 154–176. <https://doi.org/10.1016/j.engfailanal.2019.05.037>
- Ambroziak, A., Haustein, E., & Kondrat, J. (2019). Chemical and mechanical properties of 70-year-old concrete. *Journal of Materials in Civil Engineering*, 31(8), 1–7. [https://doi.org/10.1061/\(ASCE\)MT.1943-5533.0002840](https://doi.org/10.1061/(ASCE)MT.1943-5533.0002840)
- Ambroziak, A., & Malinowski, M. (2021). A 95-year-old concrete arch bridge: From materials characterization to structural analysis. *Materials*, 14(7), Article 1744. <https://doi.org/10.3390/ma14071744>
- Apanas, L., Karlikowski, J., & Siekierski, W. (2018). Ocena skutków pęknięć poprzecznic w celu określenia warunków tymczasowej eksploatacji kolejowego przęsła kratownicowego. *Archiwum Instytutu Inżynierii Lądowej*, 26, 7–18. <https://doi.org/10.21008/j.1897-4007.2018.26.01>
- Bacinskas, D., Kamaitis, Z., Jatulis, D., & Kilikevicius, A. (2013). Field testing of old narrow-gauge railway steel truss bridge. *Procedia Engineering*, 57, 136–143. <https://doi.org/10.1016/j.proeng.2013.04.020>
- Banas, A., & Jankowski, R. (2020). Experimental and numerical study on dynamics of two footbridges with different shapes of girders. *Applied Sciences*, 10(13), Article 4505. <https://doi.org/10.3390/app10134505>
- Bertolesi, E., Buitrago, M., Adam, J. M., & Calderón, P. A. (2021). Fatigue assessment of steel riveted railway bridges: Full-scale tests and analytical approach. *Journal of Constructional Steel Research*, 182, Article 106664. <https://doi.org/10.1016/j.jcsr.2021.106664>
- Bień, J., & Salamak, M. (2022). The management of bridge structures – challenges and possibilities. *Archives of Civil Engineering*, 68(2), 5–35. <https://doi.org/10.24425/ace.2022.140627>
- Boukezzi, L., Benaissa, A., Lehabab-Boukezzi, Z., & Nasser, B. (2021). Assessment of existing steel railway bridges, Algeria. *European Journal of Environmental and Civil Engineering*, 25(1), 117–131. <https://doi.org/10.1080/19648189.2018.1518792>
- Brühwiler, E., Bosshard, M., Steck, P., Meyer, C., Tschumi, M., & Haldimann, S. (2013). Fatigue safety examination of a riveted railway bridge using data from long term monitoring. *IABSE Conference, Assessment, Upgrading and Refurbishment of Infrastructures*, Rotterdam, The Netherlands, 184–185. <https://doi.org/10.2749/222137813806482986>
- Bryła, S. W. (1924). *Podręcznik budownictwa żelaznego (Iron Building Handbook)*. Księgarnia Polska Bernarda Połonieckiego. https://bcpw.bg.pw.edu.pl/Content/3991/PDF/01SBPB_wstep.pdf

- Cavadas, F., Rodrigues, C., Félix, C., & Figueiras, J. (2013). Post-rehabilitation assessment of a centenary steel bridge through numerical and experimental analysis. *Journal of Constructional Steel Research*, 80, 264–277. <https://doi.org/10.1016/j.jcsr.2012.09.020>
- Chen, W., Yan, B., Liu, X., & Jiang, Y. (2012). Research on the finite element simulation of and updating method for old riveted truss bridges. *Stahlbau*, 81(5), 419–425. <https://doi.org/10.1002/stab.201201539>
- Chmielewski, R., & Muzolf, P. (2021). Analysis of degradation process of a railway steel bridge in the final period of its operation. *Structure and Infrastructure Engineering*, 19(4), 537–53. <https://doi.org/10.1080/15732479.2021.1956550>
- Collette, Q., Sire, S., Vermes, W. J., Mesler, V. J., & Wouters, I. (2014). Experimental investigations on hot-driven structural rivets in historical French and Belgian wrought-iron structures (1880s–1890s). *Construction and Building Materials*, 54, 258–269. <https://doi.org/10.1016/j.conbuildmat.2013.12.059>
- Correia, J. A. F. O., da Silva, A. L. L., Xin, H., Lesiuk, G., Zhu, S.-P., de Jesus, A. M. P., & Fernandes, A. A. (2021). Fatigue performance prediction of S235 base steel plates in the riveted connections. *Structures*, 30, 745–755. <https://doi.org/10.1016/j.istruc.2020.11.082>
- Croft, D. N. (1996). Effects of heat treatment. In *Heat treatment of welded steel structures* (pp. 21–47). Woodhead Publishing. <https://doi.org/10.1533/9781845698812.21>
- Cywiński, Z. (1992). Zur Korrosionsrate von Baustahl in alten Brücken. *Bauingenieur*, 67(3), 147–149.
- D-64. (1955). *Normatyw Techniczny projektowania stalowych mostów kolejowych*.
- DB AG. (2000). *DS 804 Standard: Vorschrift für Eisenbahnbrücken und sonstige Ingenieurbauwerke*. Deutsche Bahn AG.
- DB Netz AG. (2010). *Directive RiL 805, Richtlinie 805.0102: Tragsicherheit bestehender Eisenbahnbrücken*. DB Netz AG.
- de Jesus, A. M. P., da Silva, A. L. L., & Correia, J. A. F. O. (2014). Fatigue of riveted and bolted joints made of puddle iron – A numerical approach. *Journal of Constructional Steel Research*, 102, 164–177. <https://doi.org/10.1016/j.jcsr.2014.06.012>
- Gheitasi, A., Michels, J., & Luo, S. (2022). Rehabilitation and retrofit design of a historic steel truss bridge in Virginia. *International Bridge Conference, IBC 22-5, USA*.
- Gocál, J., & Odrobińák, J. (2020). On the influence of corrosion on the load-carrying capacity of old riveted bridges. *Materials*, 13(3), Article 717. <https://doi.org/10.3390/ma13030717>
- Goszczyńska, B., Świt, G., & Trąpczyński, W. (2014). Assessment of the technical state of large size steel structures under cyclic load with the acoustic emission method IADP. *Journal of Theoretical and Applied Mechanics*, 52(2), 289–299. <http://jtam.pl/pdf-102163-33723?filename=Assessment%20of%20the.pdf>
- Goszczyńska, B., Świt, G., Trąpczyński, W., & Krampikowska, A. (2013). Application of acoustic emission method to assess the technical condition of the bolted bridge. *Inżynieria i Budownictwo*, 69(10), 559–562.



- Haghani, R., Al-Emrani, M., & Heshmati, M. (2012). Fatigue-prone details in steel bridges. *Buildings*, 2(4), 456–476. <https://doi.org/10.3390/buildings2040456>
- Helmerich, R. (2013). *Riveted steel bridges: Semantic management of knowledge*. Wrocław University of Technology.
- Heydarinouri, H., Nussbaumer, A., Motavalli, M., & Ghafoori, E. (2021). Strengthening of steel connections in a 92-year-old railway bridge using prestressed CFRP rods: Multiaxial fatigue design criterion. *Journal of Bridge Engineering*, 26(6). [https://doi.org/10.1061/\(ASCE\)BE.1943-5592.0001714](https://doi.org/10.1061/(ASCE)BE.1943-5592.0001714)
- Hołowaty, J. (2017). Toughness tests on steels from old railway bridges. *Procedia Structural Integrity*, 5, 1043–1050. <https://doi.org/10.1016/j.prostr.2017.07.067>
- Hołowaty, J. (2018). Properties of high tensile steels in historical railway bridges. *Construction Materials*, 171(6), 234–245. <https://doi.org/10.1680/jcoma.17.00012>
- Hołowaty, J. M., & Wichtowski, B. (2013). Properties of Structural Steel used in Earlier Railway Bridges. *Structural Engineering International*, 23(4), 512–518. <https://doi.org/10.2749/101686613X13627347099999>
- Hołowaty, J., & Wichtowski, B. (2015). Properties of steel in railway bridge constructed in 1887. *Roads and Bridges – Drogi i Mosty*, 14(4), 271–283. <https://doi.org/10.7409/rabdim.015.018>
- Hołowaty, J., & Wichtowski, B. (2022). Properties of structural steels in historical railway bridges by diagnostic tests. *Ce/Papers*, 5(4), 73–78. <https://doi.org/10.1002/cepa.1730>
- Holzinger, H., Jeschko, A., Robra, J., & Ramberger, G. (2002). Strengthening of an old arch truss bridge, Austria. *Structural Engineering International*, 12(4), 276–280. <https://doi.org/10.2749/101686602777965153>
- Imam, B., Righiniotis, T. D., & Chryssanthopoulos, M. K. (2005). Fatigue of riveted railway bridges. *Steel Structures*, 5(5), 485–494.
- ISO. (2016). *ISO 148-1 Metallic materials – Charpy pendulum impact test – Part 1: Test method*. International Organization for Standardization.
- ISO. (2019). *ISO 6892-1 Metallic materials – Tensile testing – Part 1: Method of test at room temperature*. International Organization for Standardization.
- Jakiel, P., & Bajno, D. (2018). Assessment of technical condition of historic Penny Bridge in Opole in the context of its restoration. *MATEC Web of Conferences*, 174, Article 03019. <https://doi.org/10.1051/mateconf/201817403019>
- Jang, S., Li, J., & Spencer, B. F. (2013). Corrosion estimation of a historic truss bridge using model updating. *Journal of Bridge Engineering*, 18(7), 678–689. [https://doi.org/10.1061/\(asce\)be.1943-5592.0000403](https://doi.org/10.1061/(asce)be.1943-5592.0000403)
- Jukowski, M., Beç, J., & Błazik-Borowa, E. (2018). Identification of the numerical model of FEM in reference to measurements in situ. *AIP Conference Proceedings*, 1922(1), Article 150008. <https://doi.org/10.1063/1.5019161>
- Kääriäinen, J., & Pulkkinen, P. (2002). Rehabilitation of Tornionjoki steel truss bridge, Finland. *Structural Engineering International*, 12(4), 273–275. <https://doi.org/10.2749/101686602777965207>
- Koc, W. (2021). An analytical approach to intertrack space widening on railroad curves. *Problemy Kolejnictwa – Railway Reports*, 65(193), 83–95. <https://doi.org/10.36137/1933E>

- Kołąkowski, P., Mroz, A., Sala, D., Pawłowski, P., Sekuła, K., & Świercz, A. (2013). Investigation of dynamic response of a railway bridge equipped with a tailored SHM system. *Key Engineering Materials*, 569–570, 1068–1075. <https://doi.org/10.4028/www.scientific.net/KEM.569-570.1068>
- Kołąkowski, P., Szelek, J., Sekuła, K., Świercz, A., Mizerski, K., & Gutkiewicz, P. (2011). Structural health monitoring of a railway truss bridge using vibration-based and ultrasonic methods. *Smart Materials and Structures*, 20(3), Article 035016. <https://doi.org/10.1088/0964-1726/20/3/035016>
- Kossakowski, P. G. (2013). Fatigue strength of an over one hundred year old railway bridge. *Baltic Journal of Road and Bridge Engineering*, 8(3), 166–173. <https://doi.org/10.3846/bjrbe.2013.21>
- Kossakowski, P. G. (2016). Mechanical properties of late-nineteenth-century bridge steel at low temperature. *Procedia Engineering*, 156, 180–185. <https://doi.org/10.1016/j.proeng.2016.08.284>
- Kossakowski, P. G. (2021). Mechanical properties of bridge steel from the late 19th century. *Applied Sciences (Switzerland)*, 11(2), Article 478. <https://doi.org/10.3390/app11020478>
- Kowal, M., & Szala, M. (2020). Diagnosis of the microstructural and mechanical properties of over century-old steel railway bridge components. *Engineering Failure Analysis*, 110, Article 104447. <https://doi.org/10.1016/j.engfailanal.2020.104447>
- Krawczyk, R., Słania, J., Golański, G., & Zieliński, A. (2022). Evaluation of the properties and microstructure of thick-walled welded joint of wear resistant materials. *Materials*, 15(19), Article 7009. <https://doi.org/10.3390/ma15197009>
- Kwiatkowski, J., Anigacz, W., & Beben, D. (2020). A case study on the noncontact inventory of the oldest European cast-iron bridge using terrestrial laser scanning and photogrammetric techniques. *Remote Sensing*, 12(17), Article 2745. <https://doi.org/10.3390/rs12172745>
- Łagoda, G., & Łagoda, M. (2009). Strengthening steel bridge across Vistula River in Poland. *IABSE Symposium: Sustainable Infrastructure – Environment Friendly, Safe and Resource Efficient*, Bangkok, Thailand, 156–164. <https://doi.org/10.2749/222137809796088468>
- Leander, J., Norlin, B., & Karoumi, R. (2015). Reliability-based calibration of fatigue safety factors for existing steel bridges. *Journal of Bridge Engineering*, 20(10). [https://doi.org/10.1061/\(ASCE\)BE.1943-5592.0000716](https://doi.org/10.1061/(ASCE)BE.1943-5592.0000716)
- Leonetti, D., Maljaars, J., Pasquarelli, G., & Brando, G. (2020). Rivet clamping force of as-built hot-riveted connections in steel bridges. *Journal of Constructional Steel Research*, 167, Article 105955. <https://doi.org/10.1016/j.jcsr.2020.105955>
- Lima, K., Robson, N., Oosterhof, S., Kanji, S., DiBattista, J., & Montgomery, C. J. (2008). Rehabilitation of a 100-year-old steel truss bridge. *Proceedings, Annual Conference – Canadian Society for Civil Engineering*, 4, 2408–2418. https://www.researchgate.net/publication/289063540_Rehabilitation_of_a_100-year-old_steel_truss_bridge



- Malešev, M., Radonjanin, V., Ladinović, D., Lukić, I., Šupić, S., & Draganić, S. (2016). The road steel bridge over Bosut river in Serbia Part 1: The assessment of the bridge. *Procedia Engineering*, 156, 219–226. <https://doi.org/10.1016/j.proeng.2016.08.290>
- Malinowski, M., Banas, A., Cywiński, Z., Jeszka, M., & Sitarski, A. (2017). Zur Wiedergeburt einer historischen Gitterbrücke. *Stahlbau*, 86(9), 789–796. <https://doi.org/10.1002/stab.201710523>
- Malinowski, M., Banas, A., Jeszka, M., & Sitarski, A. (2018). Imaginative footbridge in Mikolajki, Poland. *Stahlbau*, 87(3), 248–255. <https://doi.org/10.1002/stab.201810582>
- Marchewka, A., Ziółkowski, P., & Aguilar-Vidal, V. (2020). Framework for structural health monitoring of steel bridges by computer vision. *Sensors (Switzerland)*, 20(3), Article 700. <https://doi.org/10.3390/s20030700>
- Marques, F., Correia, J. A. F. O., de Jesus, A. M. P., Cunha, Á., Caetano, E., & Fernandes, A. A. (2018). Fatigue analysis of a railway bridge based on fracture mechanics and local modelling of riveted connections. *Engineering Failure Analysis*, 94, 121–144. <https://doi.org/10.1016/j.engfailanal.2018.07.016>
- Marques, F., Moutinho, C., Magalhães, F., Caetano, E., & Cunha, Á. (2014). Analysis of dynamic and fatigue effects in an old metallic riveted bridge. *Journal of Constructional Steel Research*, 99, 85–101. <https://doi.org/10.1016/j.jcsr.2014.04.010>
- Martín-Sanz, H., Tatsis, K., Damjanovic, D., Stipanovic, I., Sajna, A., Duvnjak, I., Bohinc, U., Brühwiler, E., & Chatzi, E. (2019). Getting more out of existing structures: Steel bridge strengthening via UHPFRC. *Frontiers in Built Environment*, 5, Article 26. <https://doi.org/10.3389/fbuil.2019.00026>
- Michalak, B., & Eckert, W. (2018). The historic steel bridge in Stany. Heritage preservation. Changing the function. *Civil and Environmental Engineering Reports*, 28(2), 111–123. <https://doi.org/10.2478/ceer-2018-0023>
- Nagavi, R. S., & Aktan, A. E. (2003). Nonlinear behavior of heavy class steel truss bridges. *Journal of Structural Engineering*, 129(8), 1113–1121. [https://doi.org/10.1061/\(ASCE\)0733-9445\(2003\)129:8\(1113\)](https://doi.org/10.1061/(ASCE)0733-9445(2003)129:8(1113))
- Nam, H., Yoo, J., Yun, K., Xian, G., Park, H., Kim, N., Song, S., & Kang, N. (2021). Comprehensive analysis of cold-cracking ratio for flux-cored arc steel welds using Y- and y-grooves. *Materials*, 14(18), Article 5349. <https://doi.org/10.3390/ma14185349>
- Nguyen, X. T., Nogami, K., Yoda, T., Kasano, H., Murakoshi, J., Honda, H., & Tashiro, D. (2015). Evaluation of corrosion at contact surface on gusset plate connections of steel truss bridge. *J-STAGE*, 22(85), 161–171. https://doi.org/10.11273/jssc.22.85_161
- Nowak, M., Lyasota, I., & Kisała, D. (2017). Testing the node of a railway steel bridge using an acoustic emission method. In G. Shen, Z. Wu, & J. Ahang (Eds.), *Advances in Acoustic Emission Technology*, 179, (pp. 265–275). Springer, Cham. https://doi.org/10.1007/978-3-319-29052-2_23
- Ocel, J. (2021). *Historical changes to steel bridge design, composition, and properties* (Report No. FHWA-HRT-21-020). Federal Highway Administration.

- <https://www.fhwa.dot.gov/publications/research/infrastructure/structures/bridge/21020/index.cfm>
- Pipinato, A. (2010). Step level procedure for remaining fatigue life evaluation of one railway bridge. *Baltic Journal of Road and Bridge Engineering*, 5(1), 28–37. <https://doi.org/10.3846/bjrbe.2010.04>
- Pipinato, A., Pellegrino, C., & Modena, C. (2012). Assessment procedure and rehabilitation criteria for the riveted railway Adige Bridge. *Structure and Infrastructure Engineering*, 8(8), 747–764. <https://doi.org/10.1080/15732479.2010.481674>
- PKN. (1945). *PN-B-195 Concrete and reinforced concrete structures. Structural analysis and design*. Polish Committee for Standardization.
- PKN. (1951). *PN-B-03200 Steel structures – Design rules*. Polish Committee for Standardization.
- PKN. (1982). *PN-S-10052 Obiekty mostowe – Konstrukcje stalowe – Projektowanie*. Polish Committee for Standardization.
- PKN. (1985). *PN-S-10030 Bridges. Loads*. Polish Committee for Standardization.
- PKN. (2007). *PN-EN 1991-2:2007 Eurocode 1: Actions on structures – Part 2: Traffic loads on bridges*. Polish Committee for Standardization.
- PKN. (2022). *PN-EN 15528 Railway applications – Line categories for managing the interface between load limits of vehicles and infrastructure*. Polish Committee for Standardization.
- PKP. (2015). *Id-1 (D-1) Warunki Techniczne utrzymania nawierzchni na liniach kolejowych*. PKP Polskie Linie Kolejowe S.A.
- Rakoczy, A. M. (2021). Fatigue safety verification of riveted steel railway bridges using probabilistic method and standard S-N curves. *Archives of Civil Engineering*, 67(4), 625–642. <https://doi.org/10.24425/ace.2021.138522>
- Riveiro, B., González-Jorge, H., Varela, M., & Jauregui, D. V. (2013). Validation of terrestrial laser scanning and photogrammetry techniques for the measurement of vertical underclearance and beam geometry in structural inspection of bridges. *Measurement*, 46(1), 784–794. <https://doi.org/10.1016/j.measurement.2012.09.018>
- Rules for the construction and maintenance of road bridges*. (1926). Pomorska Drukarnia Rolnicza S. A. <https://polona.pl/item/przepisy-o-budowie-i-utrzymaniu-mostow-drogowych-obowiazujace-od-1-stycznia-1926-roku,MzU0NzE1Nzg/8/#info:metadata>
- Salem, H. M., & Helmy, H. M. (2014). Numerical investigation of collapse of the Minnesota I-35W bridge. *Engineering Structures*, 59, 635–645. <https://doi.org/10.1016/j.engstruct.2013.11.022>
- Sanekata, M., Nishida, H., Nakagomi, Y., Hirai, Y., Nishimiya, N., Tona, M., Hirata, N., Yamamoto, H., Tsukamoto, K., Ohshimo, K., Misaizu, F., & Fuke, K. (2021). Dependence of optical emission spectra on argon gas pressure during modulated pulsed power magnetron sputtering (MPPMS). *Plasma*, 4(2), 269–280. <https://doi.org/10.3390/plasma4020018>
- Sangiorgio, V., Nettis, A., Uva, G., Pellegrino, F., Varum, H., & Adam, J. M. (2022). Analytical fault tree and diagnostic aids for the preservation of historical steel truss bridges. *Engineering Failure Analysis*, 133, Article 105996. <https://doi.org/10.1016/j.engfailanal.2021.105996>



- Schabowicz, K. (2021). Testing of materials and elements in civil engineering. *Materials*, 14(12), Article 3412. <https://doi.org/10.3390/ma14123412>
- Sieber, L., & Stroetmann, R. (2013). Assessment methods to avoid brittle failure of old steel structures. *Assessment, Upgrading and Refurbishment of Infrastructures*, Rotterdam, The Netherlands, 574–575. <https://doi.org/10.2749/222137813806548361>
- Siekierski, W. (2015). An efficient method for analysis of service load stresses in bridge gusset plates. *Engineering Structures*, 84, 152–161. <https://doi.org/10.1016/j.engstruct.2014.11.029>
- Siekierski, W. (2016). Analysis of gusset plate of contemporary bridge truss girder. *Baltic Journal of Road and Bridge Engineering*, 11(3), 188–196. <https://doi.org/10.3846/bjrbe.2016.22>
- Siwowski, T. (2013). The rehabilitation of long span truss bridge. *Long Span Bridges and Roofs – Development, Design and Implementation*, Kolkata, India, 1–8. <https://doi.org/10.2749/222137813808627028>
- Siwowski, T. (2015). Fatigue assessment of existing riveted truss bridges: Case study. *Bulletin of the Polish Academy of Sciences: Technical Sciences*, 63(1), 125–133. <https://doi.org/10.1515/bpasts-2015-0014>
- Siwowski, T., Zobel, H., Al-Khafaji, T., & Karwowski, W. (2020). The recently built polish large arch bridges – A review of construction technology. *Archives of Civil Engineering*, 66(4), 7–43. <https://doi.org/10.24425/ace.2020.135207>
- Stamatopoulos, G. N. (2013). Fatigue assessment and strengthening measures to upgrade a steel railway bridge. *Journal of Constructional Steel Research*, 80, 346–354. <https://doi.org/10.1016/j.jcsr.2012.10.004>
- Steffen, S., Niemann, P., & Geißler, K. (2023). Erläuterungen zur aktuell überarbeiteten Richtlinie 805 zur Bewertung von Ingenieurbauwerken der Deutschen Bahn. *Bautechnik*, 100(6), 318–333. <https://doi.org/10.1002/bate.202300044>
- Tasak, E., & Ziewiec, A. (2009). *Spawalność materiałów konstrukcyjnych tom 1 Spawalność stali*. Wydawnictwo JAK.
- Tomków, J., & Tomków, M. (2019). The influence of the carbon equivalent on the weldability of high-strength low-alloy steel in the water environment. *Welding Technology Review*, 91(5), 43–49. <https://doi.org/10.26628/wtr.v91i5.1001>
- UIC. (1986). *UIC 779-1 Z. Zalecenia do określania nośności istniejących przęseł stalowych*.
- Vélez, Á. P., Sánchez, A. B., Bruna, O. A., Abella, D. M., de Prado, L. Á., & Fernández, M. M. (2021). Material behavior and fatigue assessment of old steel bridges of the spanish conventional rail network. *Materials*, 14(18), Article 5275. <https://doi.org/10.3390/ma14185275>
- Vičan, J., Gocál, J., Odrobiňák, J., & Koteš, P. (2016). Existing steel railway bridges evaluation. *Civil and Environmental Engineering*, 12(2), 103–110. <https://doi.org/10.1515/cee-2016-0014>
- Vůjtěch, J., Ryjáček, P., Campos Matos, J., & Ghafoori, E. (2021). Iron-based shape memory alloy for strengthening of 113-year bridge. *Engineering Structures*, 248, Article 113231. <https://doi.org/10.1016/j.engstruct.2021.113231>



- Walia, S. K., Patel, R. K., Vinayak, H. K., & Parti, R. (2015). Time-frequency and wavelet-based study of an old steel truss bridge before and after retrofiting. *Journal of Civil Structural Health Monitoring*, 5(4), 397–414. <https://doi.org/10.1007/s13349-015-0116-9>
- Wang, C. S., Qian, H., Zhan, A., Xu, Y., & Hu, D. L. (2007). Fatigue and fracture evaluation of a 70 year old steel bridge. *Key Engineering Materials*, 347, 359–364. <https://doi.org/10.4028/www.scientific.net/KEM.347.359>
- Wang, C. S., Sheng, H. J., Hu, J. Y., Yan, S. L., & Duan, L. (2012). Material properties and fatigue safety evaluation of old metal bridges. *Key Engineering Materials*, 525–526, 137–140. <https://doi.org/10.4028/www.scientific.net/KEM.525-526.137>
- Wichtowski, B. (2014). Load-carrying capacity of steel railway bridges of the second half of XIX century – discussion. *Roads and Bridges – Drogi i Mosty*, 13(3), 261–269. <https://doi.org/10.7409/rabdim.014.017>
- Wichtowski, B., & Hołowaty, J. (2011). Structural steels in old railway bridges analyzed by hardness and chemical content (Analiza stali starych mostów kolejowych według badań twardości i składu chemicznego). *XXV Konferencja Naukowo-Techniczna – Awarie Budowlane*, 1259–1266.
- Yilmaz, M. F., Ozakgul, K., & Caglayan, B. O. (2022). Simulation-based reliability analysis of steel girder railway bridges. *Baltic Journal of Road and Bridge Engineering*, 17(3), 44–65. <https://doi.org/10.7250/bjrbe.2022-17.568>
- Zobel, H., Karwowski, W., Wróbel, M., & Mossakowski, P. (2016). Łazienkowski bridge fire in Warsaw – Structural damage and restoration method. *Archives of Civil Engineering*, 62(4), 171–186. <https://doi.org/10.1515/ace-2015-0104>
- Zoltowski, K., Banas, A., Binczyk, M., & Kalitowski, P. (2022). Control of the bridge span vibration with high coefficient passive damper. Theoretical consideration and application. *Engineering Structures*, 254, Article 113781. <https://doi.org/10.1016/j.engstruct.2021.113781>

Appendix A

Characteristic stress values for basic load combinations are determined and collected in Tables A1–A8 for the most stressed bridge construction elements.

Table A1. Largest characteristic stress values for loads in the basic combination with dynamic coefficient $\Phi_3 = 1.08$

Truss elements	Top chord	Bottom chord	Post	Crossed diagonal
σ , MPa	149.5	132.0	77.7	50
LM71 $\alpha = 1.0$ σ_{lim} , MPa	157.3	157.3	157.3	157.3
σ/σ_{lim} , %	95	84	49	32



Table A2. Characteristic stress values for loads in the basic combination with dynamic coefficient depending on the speed in a complex stress state for the most stressed truss elements

Truss elements		Top chord	Bottom chord	Post	Crossed diagonal
C2 $v=120$ km/h $1+\varphi=1.09$	σ , MPa	109.4	95.6	54.7	35
	σ_{lim} , MPa	157.3	157.3	157.3	157.3
	σ/σ_{lim} , %	70	61	35	22
D4 $v=80$ km/h $1+\varphi=1.07$	σ , MPa	125.2	109.7	69.2	40.5
	σ/σ_{lim} , %	80	70	44	26
D4xL $v=80$ km/h $1+\varphi=1.07$	σ , MPa	127.9	113.1	74.5	40.1
	σ/σ_{lim} , %	81	72	47	25

Table A3. Largest characteristic stress values for loads in the basic combination with dynamic coefficient $\Phi 3 = 1.08$ in a complex stress state

Truss elements	Compression with buckling					Netto cross-section tension
	Top chord	Outer diagonal	Middle diagonal	Outer post	Middle post	Bottom chord
σ , MPa	104.0	57.1	53.4	47.7	55.2	153.4
LM71 $\alpha = 1.0$ σ_{lim} , MPa	157.3	157.3	157.3	157.3	157.3	157.3
σ/σ_{lim} , %	66	36	34	30	35	98

Table A4. Characteristic stress values for loads in the basic combination with dynamic coefficient depending on the speed in a complex stress state for the most stressed truss elements

Truss elements		Compression with buckling					Netto cross-section tension
		Top chord	Outer diagonal	Middle diagonal	Outer post	Middle post	Bottom chord
C2 $v=120$ km/h $\rho=1.08$	σ , MPa	75.5	39.81	32.4	29.0	32.7	111.1
	σ_{lim} , MPa	157.3	157.3	157.3	157.3	157.3	157.3
	σ/σ_{lim} , %	48	25	21	18	21	71
$v=80$ km/h $\rho=1.08$	σ , MPa	87.0	46.2	37.6	31.6	35.7	127.6
	σ/σ_{lim} , %	55	29	24	20	23	81
$\times L v=80$ km/h $\rho=1.08$	σ , MPa	89.2	45.5	26.9	35.0	39.9	131.5
	σ/σ_{lim} , %	57	29	17	22	25	84



Table A5. Largest characteristic stress values for loads in the basic combination with dynamic coefficient $\Phi_3=1.40$ for the stringer and $\Phi_3 = 1.67$ for the cross girder

Deck elements	Stringer	Cross girder
σ , MPa	117.2	353.1
LM71 $\alpha = 1.0$ σ_{lim} , MPa	157.3	157.3
σ/σ_{lim} , %	74	224

Table A6. Characteristic stress values for loads in the basic combination with dynamic coefficient depending on the speed in a complex stress state for the most stressed deck elements

Deck elements	Stringer	Cross girder
D2 $v=120$ km/h Stringer $1+\varphi=1.40$, Cross girder $1+\varphi=1.89$	σ , MPa 95.0	269.8
	σ_{lim} , MPa 157.3	157.3
	σ/σ_{lim} , % 60	172
D4 $v=80$ km/h Stringer $1+\varphi=1.28$, Cross girder $1+\varphi=1.56$	σ , MPa 99.1	268.9
	σ/σ_{lim} , % 63	171
D4xL $v=80$ km/h Stringer $1+\varphi=1.28$, Cross girder $1+\varphi=1.56$	σ , MPa 108.8	284.3
	σ/σ_{lim} , % 69	181
C2 $v=50$ km/h Stringer $1+\varphi=1.17$, Cross girder $1+\varphi=1.32$	σ , MPa 80.8	200.0
	σ/σ_{lim} , % 51	127
D4 $v=50$ km/h Stringer $1+\varphi=1.17$, Cross girder $1+\varphi=1.32$	σ , MPa 91.3	233.3
	σ/σ_{lim} , % 58	148
D4xL $v=50$ km/h Stringer $1+\varphi=1.17$, Cross girder $1+\varphi=1.32$	σ , MPa 100.3	246.3
	σ/σ_{lim} , % 64	157

Table A7. Largest characteristic shear stress values for loads in the basic combination with dynamic coefficient $\Phi_3=1.40$ for the stringer and $\Phi_3=1.67$ for the cross girder

Deck elements	Stringer	Cross girder
τ , MPa	51.3	192.2
LM71 $\alpha = 1.0$ τ_{lim} , MPa	78	78
τ/τ_{lim} , %	66	246

Table A8. Characteristic shear stress values for loads in the basic combination with dynamic coefficient depending on the speed in a complex stress state for the most stressed deck elements

Deck elements		Stringer	Cross girder
C2 v=120 km/h	τ , MPa	39.4	149.8
Stringer 1+ φ =1.40, Cross girder 1+ φ =1.89	τ_{lim} , MPa	78	78
	τ/τ_{lim} , %	51	192
D4 v=80 km/h	τ , MPa	40.7	149.8
Stringer 1+ φ =1.28, Cross girder 1+ φ =1.56	τ/τ_{lim} , %	52	192
D4xL v=80 km/h	τ , MPa	43.4	157.3
Stringer 1+ φ =1.28, Cross girder 1+ φ =1.56	τ/τ_{lim} , %	56	202
C2 v=50 km/h	τ , MPa	33.3	111.2
Stringer 1+ φ =1.17, Cross girder 1+ φ =1.32	τ/τ_{lim} , %	43	143
D4 v=50 km/h	τ , MPa	37.4	130.1
Stringer 1+ φ =1.17, Cross girder 1+ φ =1.32	τ/τ_{lim} , %	48	167
D4xL v=50 km/h	τ , MPa	39.8	136.5
Stringer 1+ φ =1.17, Cross girder 1+ φ =1.32	τ/τ_{lim} , %	51	175